LETTERS

# Global changes to the ubiquitin system in Huntington's disease

Eric J. Bennett[1], Thomas A. Shaler[2], Ben Woodman[3], Kwon-Yul Ryu[1], Tatiana S. Zaitseva[1], Christopher H. Becker[2], Gillian P. Bates[3], Howard Schulman[2] & Ron R. Kopito[1]

**Huntington's disease (HD) is a dominantly inherited neurodegenerative disorder caused by expansion of CAG triplet repeats in the huntingtin (*HTT*) gene (also called *HD*) and characterized by accumulation of aggregated fragments of polyglutamine-expanded HTT protein in affected neurons[1,2]. Abnormal enrichment of HD inclusion bodies with ubiquitin, a diagnostic characteristic of HD and many other neurodegenerative disorders including Alzheimer's and Parkinson's diseases[3,4], has suggested that dysfunction in ubiquitin metabolism may contribute to the pathogenesis of these diseases[5,6]. Because modification of proteins with polyubiquitin chains regulates many essential cellular processes including protein degradation, cell cycle, transcription, DNA repair and membrane trafficking[7], disrupted ubiquitin signalling is likely to have broad consequences for neuronal function and survival. Although ubiquitin-dependent protein degradation is impaired in cell-culture models of HD[8–11] and of other neurodegenerative diseases[12,13], it has not been possible to evaluate the function of the ubiquitin–proteasome system (UPS) in HD patients or in animal models of the disease, and a functional role for UPS impairment in neurodegenerative disease pathogenesis remains controversial[14–16]. Here we exploit a mass-spectrometry-based method to quantify polyubiquitin chains[17] and demonstrate that the abundance of these chains is a faithful endogenous biomarker of UPS function. Lys 48-linked polyubiquitin chains accumulate early in pathogenesis in brains from the R6/2 transgenic mouse model of HD, from a knock-in model of HD and from human HD patients, establishing that UPS dysfunction is a consistent feature of HD pathology. Lys 63- and Lys 11-linked polyubiquitin chains, which are not typically associated with proteasomal targeting, also accumulate in the R6/2 mouse brain. Thus, HD is linked to global changes in the ubiquitin system to a much greater extent than previously recognized.**

Lys 48-linked polyubiquitin conjugates are the proximal substrates of proteasomal proteolysis[7], so their steady-state abundance in the cell should reflect proteasome function in cells or tissues without the use of artificial reporters. We used a ubiquitin-association domain from human ubiquilin 2 (UBQLN2, also known as PLIC-2), which we called human P2UBA[18], to capture polyubiquitin chains from lysates of HEK293 cells expressing the cytoplasmic UPS reporter NESGFP$^{u}$ (ref. 9), exposed to the irreversible proteasome inhibitor clasto-lactacystin β-lactone (Lc, Supplementary Fig. 1 and Supplementary Discussion). The captured polypeptides were eluted, digested with trypsin, and the resulting peptides and isopeptides were separated by reverse-phase liquid chromatography in line with an electrospray time-of-flight mass spectrometer (LC-ESI-TOF-MS analysis). The abundance of the Lys 48-linked ubiquitin isopeptide (LIFAGK-(GG)-QLEDGR, abbreviated to UbK48) in the digest was determined by comparison of the extracted UbK48 ion (mass-to-charge ratio, $m/z = 487.60$) to a 'spiked' internal standard consisting of the corresponding synthetic isopeptide labelled with $^{13}C$ and $^{15}N$ (Fig. 1b)[17,19,20].

This analysis revealed that the concentration of Lys 48-linked chains in cell lysates increased in proportion to the Lc concentration; this signal was eliminated by pretreatment of cell lysates with the deubiquitylating enzyme Usp2cc[21] (Fig. 1a–c). In contrast, the relative abundance of non-isopeptide-linked ubiquitin (EMF–ubiquitin), determined by subtracting the amount of human P2UBA-captured ubiquitin chains from the linear ubiquitin-derived ESTLHLVLR peptide (Fig. 1a, right), was not much affected by exposure to Lc (Fig. 1c). This increase in UbK48 relative to EMF–ubiquitin is not caused by preferential capture of Lys 48-linked chains by the human P2UBA domain, because each of the ubiquitylated species present in the human P2UBA-binding reaction is at a concentration more than tenfold lower than the experimentally determined dissociation constant for human P2UBA binding[18] (Supplementary Fig. 2 and Supplementary Discussion).

Comparison of the magnitude of increase in UbK48 intensity in HEK293 cells treated with Lc with the extent of irreversible modification of the proteasome active site, assessed *in vitro* by cleavage of the fluorogenic substrate Suc-LLVY-AMC, demonstrates that the concentration of UbK48 isopeptide correlates strongly with a loss of proteasome activity, reaching a half-maximal level at ~43% inhibition (Fig. 1d). This dose–response profile is indistinguishable from that obtained by measurement of the fluorescent UPS reporter NESGFP$^{u}$ (ref. 9) in the same cells (Fig. 1e). We conclude that cellular levels of UbK48 isopeptide can serve as a sensitive and valid tool to assess UPS impairment. This approach offers distinct advantages over previous methods in that it measures an endogenous and global parameter of UPS function and permits assessment of UPS status in any cell or tissue without the need to express an artificial reporter substrate[8,22].

To assess the effect of protein aggregation on UPS function, we measured UbK48 isopeptide levels in a mouse neuroblastoma cell line (N2a) harbouring a gene fusion between green fluorescent protein (*GFP*) and human huntingtin (*HTT*) exon 1 containing 16 glutamines (*HTTQ16GFP*) or 150 glutamines (*HTTQ150GFP*), expressed under the control of an inducible promoter[10] (Fig. 2). In control experiments, we confirmed that immunoreactive high-molecular-mass ubiquitin conjugates begin to accumulate rapidly after exposure to the proteasome inhibitor MG132 in these cell lines; as in HEK293 cells, this increase was paralleled by a rapid rise in UbK48 but not in EMF–ubiquitin (Supplementary Fig. 4). *HTT* (exon 1) expression, assessed by GFP fluorescence (Fig. 2a) or immunoblot analysis (data not shown), was low or undetectable in untreated cells.

[1]Department of Biological Sciences, Stanford University, Stanford, California 94305, USA. [2]PPD Biomarker Discovery Inc., 1505 O'Brien Drive, Menlo Park, California 94025, USA. [3]Department of Medical and Molecular Genetics, King's College London School of Medicine, London SE1 9RT, UK.

GFP intensity increased in both Q16 and Q150 cells after *HTT* (exon 1) induction, remaining diffuse in cells expressing *HTTQ16GFP* and forming multiple puncta that eventually coalesced into a single juxtanuclear inclusion body after two days in cells expressing *HTTQ150GFP* (Fig. 2a, b). The increase in *HTT* (exon 1) expression was paralleled by a much greater extensive rise in high-molecular-mass ubiquitin immunoreactivity in cells expressing *HTTQ150GFP* compared to *HTTQ16GFP* (Fig. 2c, d). Analysis of the human P2UBA-captured protein by mass spectrometry confirmed that Lys 48-linked chains increased to a much greater extent after induction of *HTTQ150GFP* compared to *HTTQ16GFP* (Fig. 2e). In cells expressing *HTTQ150GFP*, increased UbK48 levels were first detectable at one day post-induction, confirming that UPS impairment is present in cellular models of HD before the formation of microscopically detectable inclusion bodies[9]. UbK48 isopeptide levels were elevated 4–5-fold above the initial uninduced values after three days of induction, whereas the levels of EMF–ubiquitin increased more modestly (≤1.8-fold) in the same cells. These data validate the use of UbK48 isopeptide levels as a biomarker for UPS impairment in a well-characterized cellular model of HD.

To determine whether UPS function is compromised by expression of mutant *HTT in vivo* we measured UbK48 isopeptide and EMF–ubiquitin concentrations in extracts from brains of R6/2 mice, a widely used mouse model of HD[23], which express a CAG-expanded *HTT* exon 1 transgene (Fig. 3). R6/2 mice are phenotypically normal at 2 weeks of age, motor impairment can be detected from 5–6 weeks of age, and the disease phenotype is pronounced at 12 weeks (ref. 23). Mass spectrometry analysis revealed that UbK48 isopeptide levels were significantly elevated at 6 and 12 weeks of age in the cortex (Fig. 3a, c) and the striatum (Fig. 3b, c) of R6/2 mice compared to non-transgenic littermates. In contrast, total ubiquitin levels, measured by enzyme-linked immunosorbent assay (ELISA) in unfractionated cortex homogenates (Supplementary Fig. 5a) or by mass spectrometry of human P2UBA-captured material (Supplementary Fig. 5b), were only slightly affected by the *HTT* transgene. Thus, the amount of ubiquitin present in Lys 48-linked chains, expressed either as a fraction of EMF–ubiquitin (Fig. 3d) or as a fraction of total ubiquitin (Supplementary Fig. 6a), was significantly elevated in R6/2 mice at both 12 and 6 weeks of age, signifying a shift of the total ubiquitin pool into higher-order conjugates and not merely an

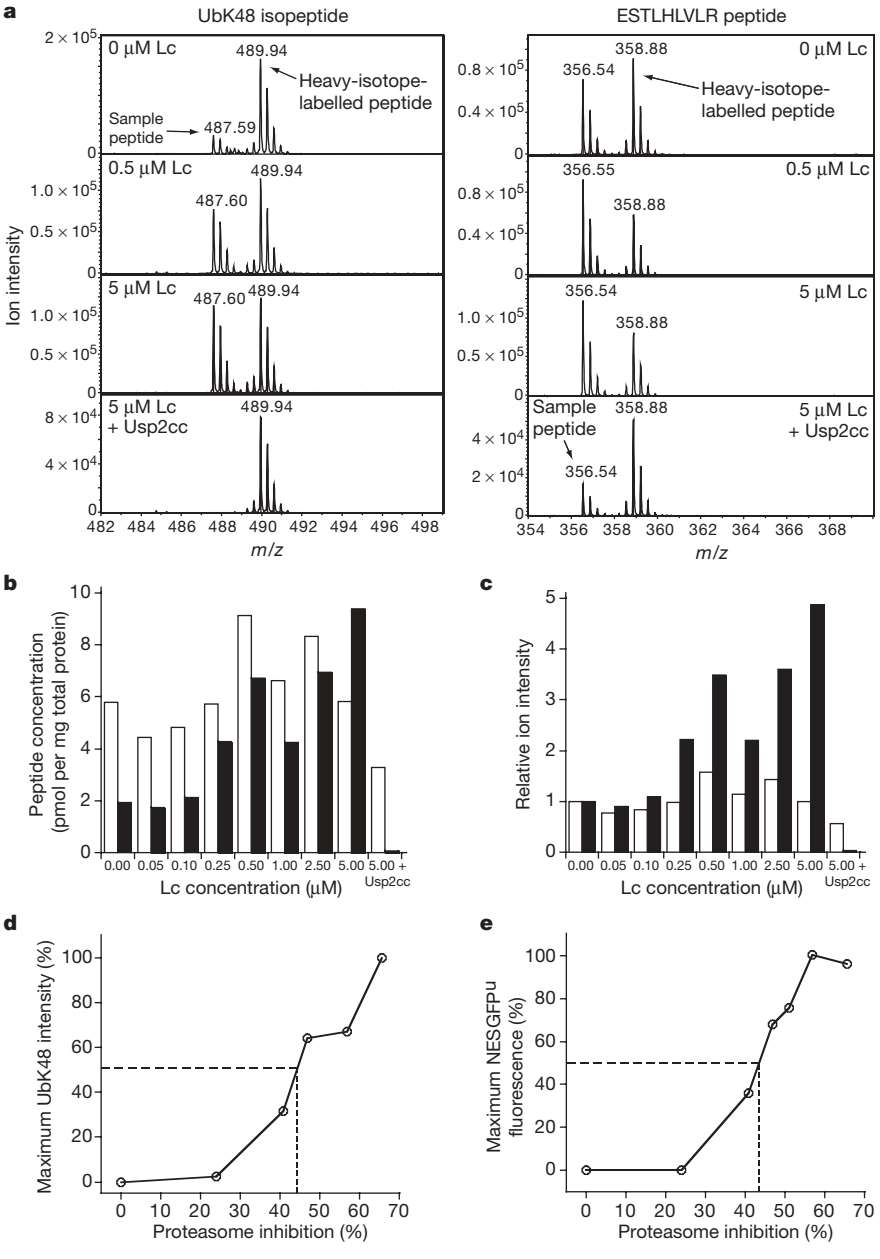


**Figure 1 | UbK48 ion intensity correlates with a loss of UPS function.** **a**, Extracted mass chromatograms of the UbK48 isopeptide (left, $m/z = 487.60$) and a linear ubiquitin peptide ESTLHLVLR (right, $m/z = 356.55$) (and their corresponding $^{13}C$, $^{15}N$ labelled standards). Ubiquitin species were captured with human P2UBA from lysates of NESGFP$^u$ HEK293 cells exposed to the indicated concentrations of Lc and were digested with Usp2cc where indicated. **b**, **c**, Absolute concentrations (**b**) and relative levels (**c**) of UbK48 isopeptide (filled bars) and non-chain ubiquitin (EMF–ubiquitin, made up of end-cap, mono-ubiquitin and free ubiquitin; open bars). **d**, **e**, Plots of relative changes in UbK48 (**d**) and NESGFP$^u$ fluorescence (**e**, measured by flow cytometry) in Lc-treated NESGFP$^u$ HEK293 cells plotted against proteasome inhibition (measured by Suc-LLVY-AMC cleavage). The dashed lines represent the half-maximal inhibition.

increase in total ubiquitin abundance. Notably, we observed a decrease in total ubiquitin (Supplementary Fig. 5), EMF–ubiquitin (Supplementary Fig. 7a) and UbK48 (Supplementary Fig. 7b) levels in mice of both genotypes between 2 and 4 weeks of age. The decline in cortical EMF–ubiquitin continued in non-transgenic mice until 12 weeks of age; this decrease was largely abrogated by 6 weeks of age in R6/2 mice (Supplementary Fig. 7a), probably offset by increased ubiquitin gene expression in response to HTT-induced UPS stress (data not shown). These data indicate that ubiquitin levels in brain are developmentally regulated.

To determine whether the observed UPS perturbation is a general feature of HD pathology, we analysed UbK48 levels in cortex homogenates from $Hdh^{Q150/Q150}$ mice at 8 and 22 months of age (where *Hdh* is the mouse orthologue of human *HTT*). These 'knock-in' mice[24] exhibit only modest levels of HTT aggregates and have variable expression of other pathological phenotypes at eight months of age[24]. However, at 22 months of age, $Hdh^{Q150/Q150}$ mice share extensive behavioural and molecular phenotypes with R6/2 mice of 12 weeks of age[25]. Consistent with this, we observed a small but significant increase in UbK48 isopeptide levels, but not in EMF–ubiquitin levels, in $Hdh^{Q150/Q150}$ mice at 22 months of age (Fig. 3e). Thus, UPS impairment is observed in two distinct, but comparable, mouse models of HD, and is not simply an artefact of overexpressed *HTT* exon 1. We also found that UbK48 isopeptide levels were elevated by 50% in the striatum and the cortex of human HD patients when compared to control, non-HD cortex (Fig. 3f). A similar elevation is also seen when HD cortex alone is compared to control cortex. This increase is specific to UbK48, because EMF–ubiquitin levels were not significantly altered in human HD brains (Fig. 3f). Thus, UPS impairment is a consistent feature of HD pathology in humans and in mouse HD models.

To investigate whether the observed perturbation of cellular ubiquitin pools by mutant *HTT* (exon 1) expression is specific for Lys 48-linked polyubiquitin chains, or whether it represents a more generalized dysregulation of ubiquitin metabolism, we exploited the same methodology to assess the impact of expression of aggregation-prone HTT protein on polyubiquitin chains that are not known to be associated with proteasomal degradation, as the human P2UBA domain is non-selective with respect to the isopeptide linkage[18] (Fig. 4). Strikingly, we observed that both UbK11 (TLTGK-(GG)-TITLEVEPSDTIENVK) and UbK63 (TLSDYNIQK-(GG)-ESTLHLVLR)

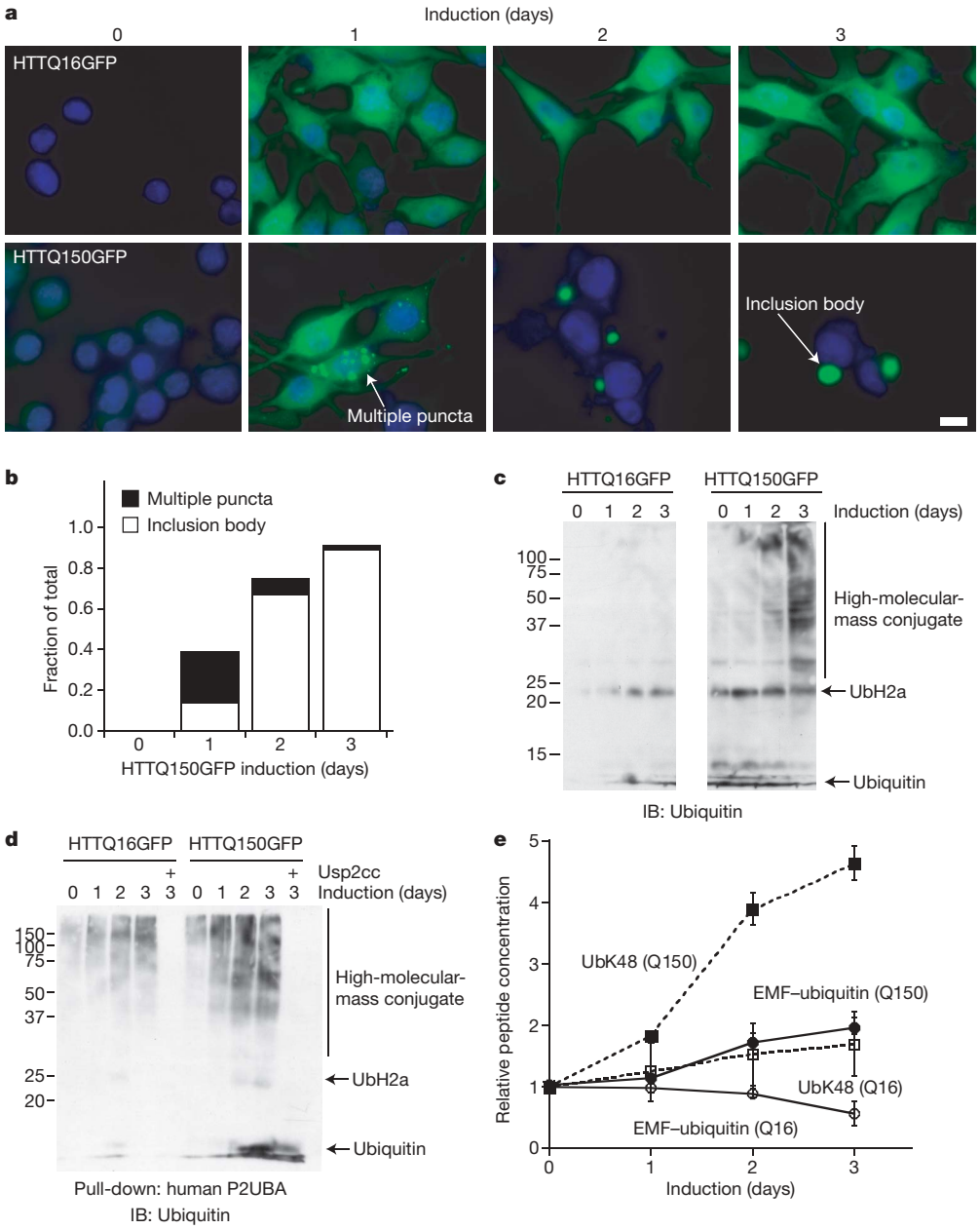


**Figure 2 | HTTQ150 aggregation in an inducible cell model of HD correlates with elevated UbK48 levels.** **a**, Fluorescence micrograph of HTTQ16GFP (top) and HTTQ150GFP (bottom) expression (green) induced for the indicated number of days. Nuclei were visualized with bisbenzimide (blue). Scale bar represents 2 μm. **b**, Quantification of HTTQ150GFP distribution scored at the positions indicated by the arrows in the representative panels of **a**. **c**, **d**, Ubiquitin immunoblot (IB) analysis of whole-cell lysates (**c**) and human P2UBA-captured protein (**d**) from cells in **a**. **e**, Relative changes in levels of the indicated ubiquitin species determined by mass spectrometry from human P2UBA pull-down assays of cells in **a** ($n = 3$). Data are presented as mean ± s.e.m.

isopeptides increased in lysates of N2a cells treated with MG132 to a relatively similar extent as did UbK48 (Fig. 4a). Although UbK11 isopeptides accumulated with similar kinetics to those of UbK48, the increase in UbK63 chains was delayed and transient. Induction of HTTQ150GFP, but not HTTQ16GFP, expression also led to an increase in the relative abundance of UbK11 and UbK63 chains (Fig. 4b), consistent with the conclusion that expression of aggregation-prone proteins globally alters ubiquitin pools. Lys 63-linked chains were also significantly elevated in homogenates from R6/2 mouse brains when expressed either as absolute isopeptide concentrations (Fig. 4d) or as relative to total ubiquitin levels (Supplementary Fig. 6b). Lys 11-linked chains showed a similar trend, but failed to reach the same level of statistical significance (Fig. 4c and Supplementary Fig. 6c). Thus, both expression of aggregation-prone proteins and direct proteasome inhibition led to alterations in polyubiquitin chains not typically associated with proteasome function. Whether these findings reflect a role for UbK63 and UbK11 chains in proteasome targeting[17,26], or perhaps in other ubiquitin-dependent processes such as trafficking to inclusion bodies or autophagy, will require further investigation.

The data reported here demonstrate that the UPS is impaired in two mouse models of HD as well as in the human disease, providing *in vivo* evidence that UPS dysfunction occurs during HD pathogenesis. The demonstration that elevated levels of polyubiquitin chains are evident in the brains of 6-week-old R6/2 mice indicates that UPS dysfunction—and its broad consequences for cellular homoeostasis—is temporally poised to contribute to the cascade of events that result in the neuronal dysfunction and death that characterize these disorders. Previous attempts to establish a definitive link between UPS impairment and neurodegenerative disease pathogenesis, first suggested from ubiquitin immunohistochemical studies as early as 1989 (ref. 4), have been hitherto hampered by the lack of

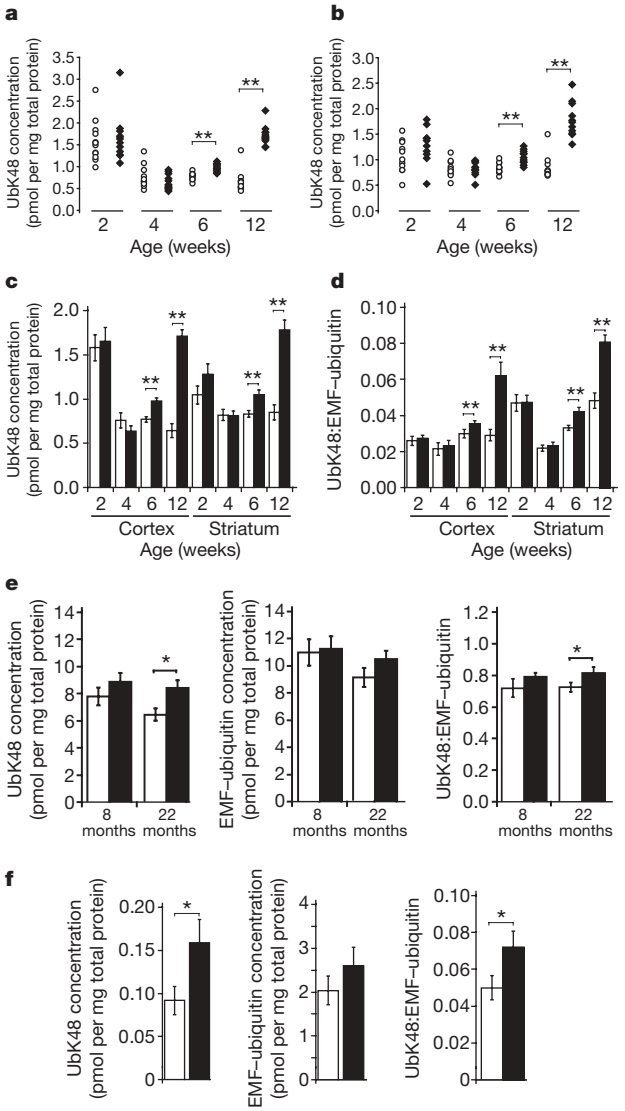


**Figure 3 | UbK48 isopeptide ion intensity is elevated in mouse models of HD and in the human HD brain.** **a**–**c**, Elevated brain Lys 48-linked polyubiquitin chain levels in a transgenic model of HD. Polyubiquitylated material from cortex (**a**) and striatum (**b**) homogenates of R6/2 mice (filled diamonds) and non-transgenic littermate mice (open circles) at the indicated ages was captured with human P2UBA. Each symbol represents an individual animal. **c**, Mean UbK48 isopeptide concentrations for R6/2 mice (filled bars) and non-transgenic littermates (open bars) ($n = 12$ for each genotype at each age). **d**, Mean UbK48:EMF–ubiquitin concentration ratio for R6/2 mice (filled bars) and non-transgenic littermates (open bars). **e**, Mean UbK48 isopeptide concentration (left panel), EMF–ubiquitin concentration (middle panel) and UbK48:EMF–ubiquitin ratio (right panel) in human P2UBA-captured cortex homogenates from *Hdh*$^{Q150/Q150}$ mice (filled bars) and age-matched non-transgenic littermates (open bars) ($n = 6$ and 8 for 8-month- and 22-month-old mice of each genotype, respectively). **f**, Mean UbK48 isopeptide concentration (left), EMF–ubiquitin concentration (middle) and UbK48:EMF–ubiquitin ratio (right) in human P2UBA-captured brain homogenates from human control (open bars) and HD (filled bars) patients ($n = 14$). All data are presented as mean ± s.e.m. Significance levels were determined using Student's *t*-test. Single asterisk and double asterisk denote $P \leq 0.05$ and $P \leq 0.01$, respectively.

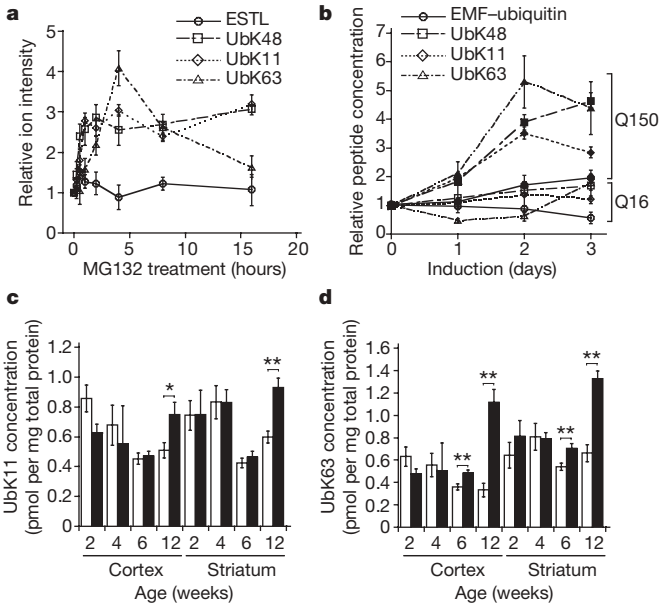


**Figure 4 | Elevated levels of polyubiquitin chain linkages not typically associated with proteasomal targeting in cellular and mouse models of HD.** **a**, Ubiquitin isopeptide levels in human P2UBA-captured material from extracts of uninduced, differentiated N2a cells exposed to MG132 (10 μM) for the indicated times. Relative ion intensities from extracted ion chromatograms were normalized to the levels of the same ions in untreated cells ($n = 3$). **b**, Ubiquitin isopeptide levels in human P2UBA-captured material from extracts of differentiated N2a cells after induction of HTTQ16GFP or HTTQ150GFP expression for the indicated times. Filled and open symbols represent data from HTTQ150GFP- and HTTQ16GFP-expressing cells, respectively. Absolute peptide concentration values were normalized to the levels in uninduced cells ($n = 3$). **c**, **d**, Concentrations of UbK11 (**c**) and UbK63 (**d**) isopeptides in human P2UBA-captured material from brain homogenates from R6/2 mice (filled bars) and non-transgenic littermates (open bars) ($n = 12$ for each genotype at each age). **b**–**d**, Reported peptide concentrations were measured using LC-ESI-TOF-MS analysis with spiked heavy-isotope-labelled standards. All data are presented as mean ± s.e.m. Significance levels were determined using Student's *t*-test. Single asterisk and double asterisk denote $P \leq 0.05$ and $P \leq 0.01$, respectively.

suitable analytic tools to assess UPS function *in vivo*. Although artificial reporters of UPS activity on the basis of destabilized GFP[8,9,11] have proved to be useful tools to probe the effects of protein aggregation on UPS activity in cell-culture models of disease, the intrinsic difficulties associated with these transgenic reporters *in vivo*[15] have precluded definitive assessment of the time course of UPS impairment relative to disease pathogenesis in animal models. The broadly applicable method described here should be useful in achieving deeper insight into the molecular basis of a wide variety of neurodegenerative diseases in humans and in animal models.

## METHODS SUMMARY

The amount of total human P2UBA-captured ubiquitin was determined as described[17] from the sum of ubiquitin in polyubiquitin chains (approximated by the sum of UbK48, UbK63 and UbK11 isopeptides) and EMF–ubiquitin (determined by subtracting the UbK48 and UbK11 concentrations from the concentration of the linear peptide ESTLHLVLR[17]). The EMF–ubiquitin value represents ubiquitin molecules that are completely unconjugated, present as mono-ubiquitin conjugates or present as the end-cap ubiquitin on a polyubiquitin chain that has a length greater than two. Although the chain and ESTL signal can come from ubiquitin chains linked by lysines other than lysines 48, 11 or 63, analysis of the ion intensities from these isopeptides in our samples reveals that they are present at levels much below those of the three main linkages (often below the level of detection) and thus do not contribute significantly to our calculations.

**Full Methods** and any associated references are available in the online version of the paper at www.nature.com/nature.

**Received 8 May; accepted 14 June 2007.**


1. MacDonald, M. E. *et al.* A novel gene containing a trinucleotide repeat that is expanded and unstable on Huntington's disease chromosomes. *Cell* **72,** 971–983 (1993).
2. Tobin, A. J. & Signer, E. R. Huntington's disease: the challenge for cell biologists. *Trends Cell Biol.* **10,** 531–536 (2000).
3. Lowe, J. *et al.* Ubiquitin is a common factor in intermediate filament inclusion bodies of diverse type in man, including those of Parkinson's disease, Pick's disease, and Alzheimer's disease, as well as Rosenthal fibres in cerebellar astrocytomas, cytoplasmic bodies in muscle, and mallory bodies in alcoholic liver disease. *J. Pathol.* **155,** 9–15 (1988).
4. Mayer, R. J., Lowe, J., Lennox, G., Doherty, F. & Landon, M. Intermediate filaments and ubiquitin: a new thread in the understanding of chronic neurodegenerative diseases. *Prog. Clin. Biol. Res.* **317,** 809–818 (1989).
5. DiFiglia, M. *et al.* Aggregation of huntingtin in neuronal intranuclear inclusions and dystrophic neurites in brain. *Science* **277,** 1990–1993 (1997).
6. Ross, C. A. & Pickart, C. M. The ubiquitin–proteasome pathway in Parkinson's disease and other neurodegenerative diseases. *Trends Cell Biol.* **14,** 703–711 (2004).
7. Pickart, C. M. & Fushman, D. Polyubiquitin chains: polymeric protein signals. *Curr. Opin. Chem. Biol.* **8,** 610–616 (2004).
8. Bence, N. F., Sampat, R. M. & Kopito, R. R. Impairment of the ubiquitin–proteasome system by protein aggregation. *Science* **292,** 1552–1555 (2001).
9. Bennett, E. J., Bence, N. F., Jayakumar, R. & Kopito, R. R. Global impairment of the ubiquitin–proteasome system by nuclear or cytoplasmic protein aggregates precedes inclusion body formation. *Mol. Cell* **17,** 351–365 (2005).
10. Jana, N. R., Zemskov, E. A., Wang, G. & Nukina, N. Altered proteasomal function due to the expression of polyglutamine-expanded truncated N-terminal huntingtin induces apoptosis by caspase activation through mitochondrial cytochrome *c* release. *Hum. Mol. Genet.* **10,** 1049–1059 (2001).
11. Verhoef, L. G., Lindsten, K., Masucci, M. G. & Dantuma, N. P. Aggregate formation inhibits proteasomal degradation of polyglutamine proteins. *Hum. Mol. Genet.* **11,** 2689–2700 (2002).
12. Petrucelli, L. *et al.* Parkin protects against the toxicity associated with mutant α-synuclein: proteasome dysfunction selectively affects catecholaminergic neurons. *Neuron* **36,** 1007–1019 (2002).
13. Urushitani, M., Kurisu, J., Tsukita, K. & Takahashi, R. Proteasomal inhibition by misfolded mutant superoxide dismutase 1 induces selective motor neuron death in familial amyotrophic lateral sclerosis. *J. Neurochem.* **83,** 1030–1042 (2002).
14. Wang, H. L. *et al.* Polyglutamine-expanded ataxin-7 decreases nuclear translocation of NF-κB p65 and impairs NF-κB activity by inhibiting proteasome activity of cerebellar neurons. *Cell Signal.* **19,** 573–581 (2007).
15. Bowman, A. B., Yoo, S. Y., Dantuma, N. P. & Zoghbi, H. Y. Neuronal dysfunction in a polyglutamine disease model occurs in the absence of ubiquitin–proteasome system impairment and inversely correlates with the degree of nuclear inclusion formation. *Hum. Mol. Genet.* **14,** 679–691 (2005).
16. Kabashi, E., Agar, J. N., Taylor, D. M., Minotti, S. & Durham, H. D. Focal dysfunction of the proteasome: a pathogenic factor in a mouse model of amyotrophic lateral sclerosis. *J. Neurochem.* **89,** 1325–1335 (2004).
17. Kirkpatrick, D. S. *et al.* Quantitative analysis of *in vitro* ubiquitinated cyclin B1 reveals complex chain topology. *Nature Cell Biol.* **8,** 700–710 (2006).
18. Raasi, S., Varadan, R., Fushman, D. & Pickart, C. M. Diverse polyubiquitin interaction properties of ubiquitin-associated domains. *Nature Struct. Mol. Biol.* **12,** 708–714 (2005).
19. Barr, J. R. *et al.* Isotope dilution–mass spectrometric quantification of specific proteins: model application with apolipoprotein A-I. *Clin. Chem.* **42,** 1676–1682 (1996).
20. Dass, C., Fridland, G. H., Tinsley, P. W., Killmar, J. T. & Desiderio, D. M. Characterization of β-endorphin in human pituitary by fast atom bombardment mass spectrometry of trypsin-generated fragments. *Int. J. Pept. Protein Res.* **34,** 81–87 (1989).
21. Baker, R. T. *et al.* Using deubiquitylating enzymes as research tools. *Methods Enzymol.* **398,** 540–554 (2005).
22. Lindsten, K., Menendez-Benito, V., Masucci, M. G. & Dantuma, N. P. A transgenic mouse model of the ubiquitin/proteasome system. *Nature Biotechnol.* **21,** 897–902 (2003).
23. Mangiarini, L. *et al.* Exon 1 of the *HD* gene with an expanded CAG repeat is sufficient to cause a progressive neurological phenotype in transgenic mice. *Cell* **87,** 493–506 (1996).
24. Lin, C. H. *et al.* Neurological abnormalities in a knock-in mouse model of Huntington's disease. *Hum. Mol. Genet.* **10,** 137–144 (2001).
25. Woodman, B. *et al.* The $Hdh^{Q150/Q150}$ knock-in mouse model of HD and the R6/2 exon 1 model develop comparable and widespread molecular phenotypes. *Brain Res. Bull.* **72,** 83–97 (2007).
26. Hanna, J. *et al.* Deubiquitinating enzyme ubp6 functions noncatalytically to delay proteasomal degradation. *Cell* **127,** 99–111 (2006).


**Supplementary Information** is linked to the online version of the paper at www.nature.com/nature.

**Acknowledgements** We are grateful to P. Howley, R. Baker and N. Nukina for reagents. We thank D. Kirkpatrick and N. Hathaway for suggestions, and J.-P. Vonsattel and the New York Brain Bank for the human brain tissue. This work was supported by a predoctoral training grant from NIGMS (E.J.B.), a small business innovation research grant from NINDS (H.S.), grants from the Huntington's Disease Society of America Coalition for the Cure, Hereditary Disease Foundation and High Q Foundation (G.P.B. and R.R.K.), and a grant from the Wellcome Trust (G.P.B.).

**Author Contributions** E.J.B., T.A.S., C.H.B., H.S. and R.R.K. devised the overall proteomic approach. E.J.B. performed all of the biochemical analyses, the pull-down assays and, together with T.A.S., obtained and analysed all the mass spectrometry data. All of the mouse breeding and dissection was performed by B.W. and G.P.B. T.S.Z. performed all experiments in Supplementary Fig. 2 and the analysis of the $Hdh^{Q150/Q150}$ knock-in mice. K.-Y.R. contributed the real-time RT–PCR data in Supplementary Fig. 3 and performed the ubiquitin ELISA on R6/2 and control mice. E.J.B. and R.R.K. wrote the manuscript. All authors discussed the results and contributed to the manuscript.

**Author Information** Reprints and permissions information is available at www.nature.com/reprints. The authors declare competing financial interests: details accompany the full-text HTML version of the paper at www.nature.com/nature. Correspondence and requests for materials should be addressed to R.R.K. (kopito@stanford.edu).

## METHODS

**Reagents.** MG132 and Lc were purchased from Affiniti. RapiGest was purchased from Waters. Monoclonal ubiquitin antibody was obtained from Chemicon (MAB1510). Sequencing grade trypsin was purchased from Promega. $^{13}C$, $^{15}N$ labelled peptides and isopeptides were synthesized by Cell Signaling Technology.

**Plasmids.** The ubiquitin-association domain of human PLIC-2 (amino acids 575–624) was amplified from a full-length human PLIC-2 construct by PCR and cloned into the pet21a bacterial expression vector (Novagen).

**Mice.** The R6/2 colony was maintained by backcrossing R6/2 males to (CBA × C57Bl/6) $F_1$ females (B6CBAF1/OlaHsd, Harlan Olac). Mouse husbandry, genotyping and CAG-repeats sizing were performed as previously described[25]. The CAG-repeat size of the R6/2 mice used in this study was (195.5 ± 5.8). The $Hdh^{Q150/Q150}$ knock-in mice[24] were maintained and bred as described[25].

**Protein purification.** The human PLIC-2 UBA-his6 protein (human P2UBA) was purified using NiNTA resin (Qiagen) and coupled to Affigel-10 agarose (BioRad) using the manufacturer's guidelines. The human P2UBA concentration was ~1 mg ml$^{-1}$ on the resin after coupling. The Usp2cc was expressed and purified as previously described[21].

**Cell lines.** HEK293 cells stably expressing the NESGFP$^{u}$ reporter were described previously[9]. N2a cells were maintained and induced as previously described[10].

**Microscopy.** Cells grown on polylysine-coated coverslips were fixed with 4% paraformaldehyde. DNA was stained by 10 μg ml$^{-1}$ bisbenzimide. Images were acquired with a Zeiss Axiovert 35 microscope with a ×100 objective.

**Proteasome activity assay.** Proteasome activity was measured from cell lysates essentially as described[27].

**Quantitative real-time RT–PCR.** Ten nanograms total RNA was used as a template for real-time PCR with reverse transcription (RT–PCR). We used iScript one-step RT–PCR with SYBR green kit (BioRad) and iCycler system with iCycler iQ software ver 3.1 (BioRad). The transcript levels of UbC, UbB, UbA52 and UbA80 were normalized to the level of 18S ribosomal RNA. The primers used for real-time RT–PCR were as follows: UbC-F, 5′-GTTACCACCAAGAAGGTC-3′; UbC-R, 5′-GGGAATGCAAGAACTTTATTC-3′; UbB-F, 5′-CACTGAGCTCAGTGACGAGAG-3′; UbB-R, 5′-CACGAAGATCTGCATTTTGAC-3′; UbA52-F, 5′-GTCAGCTTGCCCAGAAGTAC-3′; UbA52-R, 5′-ACTTCTTCTTGCGGCAGTTG-3′; UbA80-F, 5′-TGGCAAAATTAGCCGACTTCG-3′; UbA80-R, 5′-AACACTTGCCACAGTAATGCC-3′; 18S rRNA-F, 5′-CGGCTACCACATCCAAGGAA-3′; and 18S rRNA-R, 5′-GCTGGAATTACCGCGGCT-3′. Control plasmid DNA was generated by subcloning each complementary DNA fragment into pCR2.1 vector (Invitrogen), and $10^8$ to $10^3$ copies of plasmid DNA was used as a standard.

**Polyubiquitin affinity capture.** Cells were lysed in 1% Triton X-100, 150 mM NaCl, 20 mM Tris, pH 8.0, and complete protease inhibitor tablets (Roche). One milligram of protein was diluted to a final volume of 300 μl in IP buffer (10 mM Hepes, pH 7.2, 0.5% Triton X-100 and 150 mM NaCl), to which 75 μl human P2UBA resin (1:1 slurry) was added and incubated at 4 °C for 5 h with constant rotation. The beads were collected by centrifugation, washed twice with IP buffer and twice in cold PBS. Protein was eluted in 50 μl SDS sample buffer for immunoblot analysis or with 50 μl 0.1% RapiGest in 50 mM ammonium bicarbonate, pH 7.8, for mass spectrometry analysis. We observed that addition of 5 mM *N*-ethylmaleimide to the cell lysis buffer to reduce deubiquitylating enzyme activity increased the total intensities of all ubiquitin peptides without altering their respective proportions, as described above.

**Tissue preparation.** Dissected mouse cortex and striatum were mixed with 300 μl IP buffer and homogenized using a Teflon micro-rotator homogenizer with three ten-second pulses. The sonicated lysates were centrifuged for 5 min at 14,000*g* at 4 °C. Human HD and control post-mortem cortex and striatum were obtained from the New York Brain Bank at Columbia University. Details of ages and genders of HD and control donors are provided in Supplementary Table 1. Dissected brain regions were mixed with 5 ml IP buffer, homogenized using a glass–glass Dounce homogenizer and prepared as above.

**Sample preparation for mass spectrometry.** RapiGest eluted material was mixed with 10 pmol of heavy-isotope-labelled peptide. The eluate was incubated with 1 μg sequencing grade trypsin at 37 °C for 16 h. The trypsin digestion was then mixed with 1 μl 1 M hydrochloric acid for 30 min at 37 °C.

**Mass spectrometry.** The digested samples were analysed on a LC-MS system that consisted of an ESI-TOF mass spectrometer (MicroTOF System, Bruker Daltonics) coupled to a capillary HPLC (Agilent). The peptide mixtures were separated on a 0.32 mm inner diameter × 150 mm length C-18 reversed-phase column at a flow rate of approximately 10 μl min$^{-1}$ using a linear gradient of acetonitrile (0% to 40%) over 110 min. Eluant from the column was directly electrosprayed into the source of the mass spectrometer at a spray voltage of approximately 4 kV. To identify the peptides, a second portion of each sample was analysed by an undirected LC-MS/MS analysis on a linear ion-trap mass spectrometer (LTQ, ThermoElectron) using the same chromatography conditions as those used in the LC-MS profiling analyses. The acquired MS/MS spectra were searched against a database of protein sequences using a commercial software package (model Mascot, Matrix Sciences). Absolute quantification was performed using the ion intensities of the tracked endogenous peptides relative to the spiked labelled peptides. The ions that were tracked were: LIFAGK-GG-QLEDGR (UbK48) isopeptide unlabelled ($m/z = 487.60$) and heavy-isotope-labelled ($m/z = 489.94$), ESTLHLVLR (ESTL) peptide unlabelled ($m/z = 356.55$) and heavy-isotope-labelled ($m/z = 358.88$), TLTGK-(GG)-TITLEVEPSDTIENVK (UbK11) isopeptide unlabelled ($m/z = 801.43$) and heavy-isotope-labelled ($m/z = 803.43$), and TLSDYNIQK-(GG)-ESTLHLVLR (UbK63) isopeptide unlabelled ($m/z = 561.81$) and heavy-isotope-labelled ($m/z = 563.56$). The peak heights (intensity) of the molecular ions were used at the chromatographic peak maxima for relative quantification. Approximately 40% of total eluted material was injected into the mass spectrometer. Negligible background was observed under all circumstances at the positions of the endogenous and labelled peptides. Signal-to-noise ratios of the labelled peptides at their spike concentrations were ~300. A dynamic range approaching 10,000 was available for the experiment, although typically only a dynamic range of 1,000 was used. The limit of detection was estimated to be approximately 25 fmol mg$^{-1}$ of extracted protein and was similar for all the peptides used.

**Statistical analysis.** All data are presented as mean ± s.e.m. Significance levels were determined using Student's *t*-test. Single asterisk and double asterisk denote $P \leq 0.05$ and $P \leq 0.01$, respectively.

**Ubiquitin ELISA.** Total ubiquitin concentrations were measured as described[28].

27. Kisselev, A. F. & Goldberg, A. L. Monitoring activity and inhibition of 26S proteasomes with fluorogenic peptide substrates. *Methods Enzymol.* **398**, 364–378 (2005).
28. Ryu, K. Y., Baker, R. T. & Kopito, R. R. Ubiquitin-specific protease 2 as a tool for quantification of total ubiquitin levels in biological specimens. *Anal. Biochem.* **353**, 153–155 (2006).